Fuel 307 (2022) 121788

Contents lists available at ScienceDirect

Fuel

journal homepage: www.elsevier.com/locate/fuel

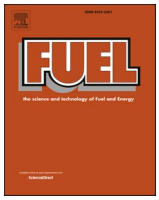

Full Length Article

Compatibility studies between an indirect injection diesel injector and biodiesel with different composition: Stationary tests

A. Alcántara-Carmona [a], F.J. López-Giménez [b], M.P. Dorado [a,*]

[a] Department of Physical Chemistry and Applied Thermodynamics, Ed Leonardo da Vinci, Campus de Rabanales, Universidad de Córdoba, Campus de excelencia internacional agroalimentario, ceiA3, 14071 Córdoba, Spain
[b] Department of Rural Engineering, Ed Leonardo da Vinci, Campus de Rabanales, Universidad de Córdoba, Campus de excelencia internacional agroalimentario, ceiA3, 14071 Córdoba, Spain

ARTICLE INFO

Keywords:
Biofuel
Metal alloy
Material deterioration
Acid value
Oxidation
Corrosion

ABSTRACT

Compatibility between automotive materials and biodiesel is key for engine manufacturers, since failures occur in the medium term and may significantly reduce engine useful life. There are only few studies about compatibility between biodiesel and pure materials, but all agree there is biodiesel degradation and material corrosion beyond desirable values. This manuscript shows results about the compatibility behavior of an indirect injection diesel engine injector, with different types of biodiesel (from rapeseed, soybean, coconut and palm oil). Tests were carried out by static immersion of actual injector parts inside biodiesel, at room temperature, during 1100 h. To analyze elemental composition of each injector part and potential compatibility problems, scanning electron microscope (SEM) and energy-dispersive X-ray spectroscopy (EDS) were used. Visual variations were detected in both biodiesel and metals, showing the need of a further quantification of both piece mass loss and biodiesel acid value increase. Metallic oxides on the surface were detected by X-ray photoelectron spectroscopy (XPS). After immersion tests, mass variation in alloying elements of each piece (behaving differently depending on their composition), besides biodiesel acid value differences, were found. In this sense, pieces with aluminum alloys showed the highest corrosion (mass loss) compared to those without aluminum in their structure, no matter the unsaturation degree and chain length of biodiesel. In sum, there were not conclusive results about the influence of biodiesel composition over injector materials. However, it was found that European biodiesel standard EN 14214 should include other parameters than just copper band corrosion, to determine material deterioration, provided that aluminum alloys and other metals react with biodiesel.

1. Introduction

Biodiesel, as a mixture of esters, is considered chemically stable and has many properties that make it a suitable fuel, i.e. high flash point and good lubricating properties compared to fossil diesel fuel. However, other properties, such as degradation of some polymers and corrosion of metallic materials, which can be in contact with biodiesel, are far from what is expected from an ideal fuel. In this context, it is important to mention that biodiesel behaves differently depending on its composition [1–3]. In this sense, the ideal biodiesel fatty acid composition includes a significant content of monounsaturated fatty acids (i.e. oleic and palmitoleic acids) and minimal presence of polyunsaturated and saturated fatty acids [4]. For this reason, it can be inferred that the influence of biodiesel over engine components may also depend on fatty acid composition. Moreover, when biodiesel oxidation is accelerated, an increase in biodiesel kinematic viscosity (ν) and density (ρ) appears. Oxidation causes formation of sediments and salts that clog filters and produce dirty injectors, among other effects, as well as the degradation and corrosion of engine components [5–8].

Considering diesel engine fuel system, the components that come in contact with fuel are fuel tank, lines, filters, injection pump, injectors, valves, cylinder heads, shirts and piston heads. For this reason, the study of compatibility between biodiesel and diesel engine fuel system materials is extremely important.

The compatibility of biodiesel with some elastomers, commonly used in the automotive industry, which are constantly in contact with fuels, i.e. nitrile rubber (NBR) has been studied [9]. Under certain conditions and periods of operation, o-rings from fluorocarbon elastomer (FKM),

* Corresponding author.
E-mail address: pilar.dorado@uco.es (M.P. Dorado).

https://doi.org/10.1016/j.fuel.2021.121788
Received 19 May 2021; Received in revised form 17 August 2021; Accepted 22 August 2021
Available online 2 September 2021

nitrile rubber (NR) and silicone rubber (SR) materials have also been tested and mass, volume and thickness changes were observed. FKM turned out to exhibit the best physical and chemical resistance. In dynamic fuel flow, SR deteriorated faster than NBR and FKM [10]. Some authors have studied the potential filter clogging due to the use of palm oil biodiesel blends, finding premature deterioration when straight biodiesel was used [11].

Research about the influence of diesel fuel and its blends with biodiesel, from both jatropha and palm oil, over engine lubricating oil has also been carried out. Results have shown that 20% biodiesel/diesel fuel blends decreased viscosity and increased engine oil acidity, thus leading to slight increase of friction and wear losses, corrosivity and oxidation of oil samples [12]. Other researchers have proposed to minimize the impact of biodiesel on lubricating oil quality through the use of detergent additives for motor oil [13].

On the other hand, many parts of the fuel system of an engine are composed by sets of different metallic materials which can be altered by water, acids and even by microorganisms present in the fuel [14–18]. The process of corrosion of metal surfaces exposed to biodiesel has been attributed to chemical corrosion, being fatty acid salts or metal oxides the main products of corrosion, depending on the metal under study [19]. Corrosion can be reduced by increasing the amount of fossil diesel fuel, in case biodiesel is blended with ultra-low sulfur diesel fuel (ULSD) [20] or by using corrosion inhibitors or antioxidants [14–16].

European standard EN ISO 2160 and American standard ASTM D130 establish a method to perform corrosiveness to copper tests from petroleum-derived products, that may be applied to biodiesel. Although both standards only consider copper corrosion, it is important to notice that, in an engine, there are different metallic and nonmetallic materials (that standards do not reference) which may also be affected by the presence of biodiesel and should not be neglected.

In car engines, components of the fuel injection pump, some filters, joints, injectors and combustion chamber are made of alloys that include copper. Alloys and compounds of Cu and Fe act as catalysts to decompose biodiesel, as they favor various chemical reactions. It has also been studied that metals, such as brass and aluminum, behave as catalysts for the oxidation of biodiesel [14,21]. It has been found that within a range, high corrosion rates occur at high temperatures [22]. Regarding stainless steel, it has been shown that it is less reactive with biodiesel compared to other metals, but also affects fuel properties [18].

Although there are parts of the fuel system and the engine that can be studied using immersion tests, new recent compatibility studies between biodiesel and materials in working engines (dynamic tests) are gaining attention [23–25]. However, these new tests only show results about a general effect on the engine, with no information about particular damaged parts. For this reason, engines and fuel systems would need to undergo subsequent static immersion tests to distinguish the incidence of the tested fuel over particular parts.

Many authors have studied compatibility of biodiesel with commercial pure metals or preforms [17,19,20,22], but to the best of our knowledge, there are only few studies based on actual parts. These parts are mostly metal alloys, that are also affected by processes of forming, heat treatment, surface treatment and other manufacturing techniques that may further affect their reactivity with biodiesel. This leads to the need of a deeper study of the compatibility of different biodiesel with different engine fuel system materials. It is essential to reach a compromise regarding fuel compatibility, considering storage and distribution systems, engine materials or other consumer devices. Also, there is very limited information on corrective measures.

Considering research carried out to date, the study of metal corrosion, elastomer degradation and fuel residues in the lubricating oil can provide generic information about global engine wear, but it does not unequivocally identify the engine part where the compatibility problem occurs and its intensity. For these reasons, the aim of this study is to test the interaction of biodiesel (showing different fatty acid composition) with materials from an indirect injection engine injector, considering exposure time, under steady-state conditions, at room temperature. This study will help manufacturers to better understand engine behavior when it is fueled with biodiesel, and potential interaction with biodiesel when vehicles are parked.

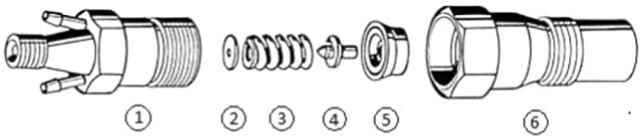

Fig. 1. Studied pieces of indirect injector. No. 1: injector housing; no. 2: stabilizing ring; no. 3: injector flat and spring; no. 4: pressure bolt; no. 5: intermediate collector of the injector; no. 6: canal and injector needle.

2. Materials and methods

2.1. Materials

2.1.1. Vegetable oils

To produce biodiesel, rapeseed oil (RO), soybean oil (SO), coconut oil (CO) and palm oil (PO) were used. Vegetable oils were provided by Instituto de Formación Agraria y Pesquera (IFAPA, Córdoba, Spain), Guinama (Alboraya, Valencia, Spain), Acofarma (Terrassa, Barcelona, Spain) and Químics Dalmau (Barcelona, Spain), respectively.

2.1.2. Reagents

For biodiesel production through transesterification, potassium hydroxide (85% purity) and methanol (99.9% purity) were acquired from Panreac (Barcelona, Spain). To analyze biodiesel acid value, PA absolute ethanol, diethyl ether stabilized with 6 ppm of BTH PA-ACS, 10 g/L phenolphthalein solution and potassium hydroxide (85% purity), PA-ACS water, all supplied by Panreac (Barcelona, Spain), were used as reagents. To determine water content, an anodic solution consisting of sulfur dioxide, imidazole and potassium iodide, using methanol as solvent, besides a cathodic solution were used. Reagents were purchased from Sigma-Aldrich (Steinheim, Germany). Hexane and sodium methylate, from Panreac (Barcelona, Spain), were used for fatty acid determination. Finally, to clean and degrease metallic parts, distilled water and acetone, respectively, were used.

2.1.3. Oil and biodiesel chemical analysis

A Perking Elmer gas chromatograph model Clarus 500, with a flame ionization detector (GC-FID), was used (Shelton, Connecticut, US). ASGE BPX70 capillary column (30 m length, 0.32 mm inner diameter and 0.25 μm film) was selected. Water content was determined by means of a Karl Fischer Coulometer DL32, accuracy of 0.1 mg (Schawerzenbach, Switzerland). Flash point was measure dusing a Seta Flash series 3 plus (sensor accuracy 0.1 mV; resistance thermometer accuracy 0.5 °C), from Instrumentación Analítica (Madrid, Spain). To measure high calorific value, calorimeter bomb IKA C200, resolution of 0.0001 °C (Ponteranica, Italy) was used. Density and viscosity were measured using a Proton 70080 densitometer and Canon-Fenske routine viscometer model 4882, size 200, respectively (accuracy of 0.2% for both instruments).

2.1.4. Engine injector

Corrosion tests were performed in a Bosch KCA 30 S 79 068 130 202 injector type (indirect injection diesel engine), manufactured in France. Pieces were cut using a metallographic cutting machine Metkon Metacut 302, from IZASA Scientific (Barcelona, Spain). Then, they were polished using a metallographic polisher Metkon Forcipol 102 from IZASA Scientific (Barcelona, Spain), using abrasive paper of silicon carbide (400 and 1200 μm) to provide a fine surface finish. Injectors are mainly made of stainless steel with different composition and treatment. Cut pieces have been named as follows: piece no. 1 (injector housing), piece no. 2

Table 1
Biodiesel optimal reaction parameters.

Oil/Fat	Catalyst (% w/w)	Alcohol-to-oil molar ratio	Temperature (°C)	Reaction time (min)
Rapeseed	1.7	6.6:1	60	60
Soybean	1.8	6.2:1	65	40
Coconut	1.5	6:1	60	50
Palm	1.5	6:1	60	50

(stabilizing ring), piece no. 3 (injector spring), piece no. 4 (pressure bolt), piece no. 5 (disk or intermediate collector of the injector) and piece no. 6 (canal and injector needle), as shown in Fig. 1.

2.1.5. Scanning electron microscope and X-Ray photoelectron Spectrometry analysis

Characterization and analysis of metal pieces were performed using JEOL JSM 7800F Scanning Electron Microscope/Energy-dispersive X-ray spectroscopy (SEM/EDS) unit and X-Ray Photoelectron Spectrometry (XPS) PHOIBOS 150 MCD unit from SPECS, respectively. Both instruments were located at the University Research Support Central Service (SCAI). EDS analysis generally provides a qualitative spectrum that shows the elements that are present in each sample.

2.2. Methods

2.2.1. Biodiesel production

Biodiesel was produced in batch, following previous optimization studies [26,27]. Optimal reaction parameters are shown in Table 1. Oil was preheated in a water bath to reach reaction temperature. Meanwhile, catalyst (KOH) and alcohol (methanol) were mixed and magnetically stirred at room temperature. Afterwards, solution was added to heated oil, keeping reaction temperature and stirring during reaction time. Once reaction was completed, it was stopped and products were let to decant. Upper phase (biodiesel) was washed with distilled water and dried with anhydrous sodium hydroxide. Resulting biodiesel was named as rapeseed oil methyl ester (ROME), soybean oil methyl ester (SOME), coconut oil methyl ester (COME) and palm oil methyl ester (POME).

2.2.2. Characterization of vegetable oil and biodiesel samples

ρ and **ν** were determined according to EN ISO 3675 and EN ISO 3104, respectively. Acid value and water content were measured following ISO 660 and EN ISO 12937, respectively. Flash point was determined considering standard EN ISO 2719. High calorific value was measured following ASTM D240 standard. Fatty acid content was calculated by GC-FID, following EN 14103 standard.

2.2.3. Characterization of metal pieces

Pieces were analyzed and classified before static immersion tests, according to UNE-EN 10020: 2001 standard (definition and classification of grades of steel). Preliminary tests suggested that, after immersion tests, pieces immersed in ROME and SOME should be further analyzed, for being the most and less outstanding in terms of acid value increase, respectively.

2.2.4. Preparation of metal samples

Injector pieces were cut using a metallographic cutting machine with a water-cooling system and slow advance, to avoid changes in metallic surfaces. Samples were washed with water and surfaces were mechanically polished by means of a polisher, using abrasive paper. Samples were quickly washed with distilled water and degreased with acetone. Then, they were dried with compressed air and placed into glass jars filled with biodiesel. Test preparation, from piece polishing to static immersion, did not exceed 10 min. Once immersion tests were finished, injector samples were removed from the solution by the aid of a magnetic rod, to avoid biodiesel contamination from outside.

Table 2
Vegetable oil chemical composition

Fatty acid/Property	RO[5]	SO[6]	CO[7]	PO[8]
Fatty acid composition (%)				
Caprylic (C8:0)	0	0	9.5	0
Decanoic (C10:0)	0	0	8	0
Lauric (C12:0)	0	0	41	0.5
Myristic (C14:0)	0	0.05	18	1.5
Palmitic (C16:0)	3.87	11.05	9	45.5
Stearic (C18:0)	2.12	3.87	3.8	4
Oleic (C18:1)	66.73	25.85	7.5	38
Linoleic (C18:2)	17.19	52.83	2.7	10
Linolenic (C18:3)	10.09	6.55	0.5	0.5
Arachidic (C20:0)	0	0.2	0	0
Behenic (C22:0)	0	0.2	0	0
Hydrocarbon chain properties				
LC (%)[1,9]	17.92	17.89	13.37	17
TUD (%)[2,10]	131.38	151.16	14.4	59.5
PUD (%)[3]	64.65	125.31	6.9	21.5
MUD (%)[4]	66.73	25.85	7.5	38

[1] Length of chain (LC).
[2] Total unsaturation degree (TUD).
[3] Polyunsaturation degree (PUD).
[4] Monounsaturation degree (MUD).
[5] RO (rapeseed oil).
[6] SO (soybean oil).
[7] CO (coconut oil).
[8] PO (palm oil).
[9] LC = $\Sigma(nC_n/100)$, where n is the number of carbon atoms of each fatty acid and C_n is the weight (in percentage) of each methyl ester in that fatty acid.
[10] TUD = (1%MU + 2%DU + 3%TU), where %MU, %DU and %TU is the weight (in percentage) of mono-, di- and triunsaturated methyl esters, respectively.

Table 3
Biodiesel characterization.

Property	Standard	ROME [1]	SOME [2]	COME [3]	POME [4]
Kinematic viscosity, ν (mm^2/s) at 40 °C	UNE EN ISO 3401 Min: 3.5; Max: 5	4.2	3.9	3.2	4.7
Density, ρ(kg/m^3) at 15 °C	UNE EN ISO 3675 Min: 860; Max: 900	884	884	897	890
Acid value (mgKOH/g)	UNE EN ISO 660 Max: 0.5	0.376	0.306	0.106	0.046
Water content (ppm)	UNE EN ISO 12937 Max: 500	303.2	412.2	485.1	463.3
Flash point (°C)	UNE EN ISO 2719 Min: 120	175.5	169	108	131.5
High calorific value (kJ/kg)	ASTM D240	39786.3	39683.6	38064.6	38,338

[1] ROME (rapeseed oil methyl ester).
[2] SOME (soybean oil methyl ester).
[3] COME (coconut oil methyl ester) and
[4] POME (palm oil methyl ester).

2.2.5. Static immersion tests

A set of glass jars, keeping selected injector pieces immersed in different types of biodiesel (ROME, SOME, COME and POME), at room temperature, for a total of 1100 h, was studied. A constant temperature water bath was used. Before and after the tests, pieces were weighed and acid value of each type of biodiesel was analyzed. Variation of these

Table 4
Elemental composition data and weight for each piece before static immersion tests

Element	Pieces [1] P1	P2	P3	P4	P5	P6
	Weight (% w/w)					
C	7.22	7.74	9.03	5.65	7.23	3.98
Mg			0.17			
Al		0.82		3.46		
Si	0.34	0.72	1.42	0.46		0.29
P			0.18	0.12	0.15	
S	0.17			0.09	0.11	
Ti				0.17		
Cr	0.23		0.64	0.29	0.09	1.48
Mn	0.82	0.65	0.75	0.50	0.57	1.42
Fe	91.47	85.96	86.48	88.55	91.58	93.41

[1] Pieces no. 1 to 6: injector housing, stabilizing ring, injector spring, pressure bolt, injector intermediate collector and canal and injector needle, respectively.

properties is indicative of changes in both metal pieces and biodiesel, which is linked to compatibility issues.

3. Results and discussion

Oil and biodiesel chemical composition, physical and chemical properties were analyzed. Results are shown in Tables 2 and 3. European biodiesel standard thresholds are included in Table 3. According to Table 2, length of chain was similar to most oils, with the exception of CO, that exhibited the lowest value. CO and PO depict the lowest degree of unsaturation. Considering Table 3, COME and POME shown the lowest acid value and the highest water content. Biodiesel, in all cases, complied with European standard, regarding ν, ρ, acid value, water content and flash point (excepting COME, for viscosity and flash point).

3.1. Visual evaluation

Once 1100 h-immersion tests were finished, changes in biodiesel color and the presence of bites on injector piece metal surfaces were observed by the naked eye. Changes in biodiesel color are shown in Supplementary material (Figures A to D). As may be seen, tone change was clearly observed in jars with pieces versus blank one. Piece no. 1 darkened biodiesel in all cases, followed by pieces no. 3, 4 and 5. In ROME and SOME, the highest differences in tone were provided by pieces no. 1, 3 and 5, while in POME, piece no. 1 showed the highest tone change. COME produced less pitch changes.

Considering tone change as an indicator of interaction, it may be inferred that biodiesel with higher unsaturation degree (i.e. ROME and SOME) may lead to compatibility issues. Regarding the chain length, COME, composed by shorter chains, underwent fewer changes in tonality, thus indicating it behaves better with any of the tested materials.

3.2. Characterization of metal samples by SEM / EDS

Material classification was achieved through a combination of image morphology, provided by SEM and material elemental composition, performed by EDS. Results shown that each injector piece consists of a different steel alloy; injector piece elemental composition is shown in Table 4.

As may be seen from Table 4, the quantity of C exceeded the amount that can be dissolved in Fe (0.05% to 0.25% of C). This is mainly due to environmental contamination. In any case, alloy element presence never exceeded 5%, thus meaning metals consisted in low-alloy steels, according to UNE-EN 10020: 2001 standard. The presence of Cr, which improves resistance to wear and corrosion, did not exceed 10%, thus meaning that metals cannot be considered stainless steels. All pieces included Mn, a basic element used to remove oxides and sulfides. Considering pieces individually, piece no. 1 included Si, S, Cr and Mn. In this context, S is usually considered an impurity, although due to the quantity found, it may be part of sulfides, that works as internal lubricant, allowing high machinability. Piece no. 2 shows Al, Si and Mn. Al and Si are used to remove oxides in steel. In addition, Si works as a hardener. Piece no. 3 presents Mg, Si, P, Cr and Mn. The amount of Si and Mn (approx. 1.4% Si and 1% Mn) turns it into a suitable spring steel. Piece no. 4 showed Al, Si, P, S, Ti, Cr and Mn. The presence of Ti, also

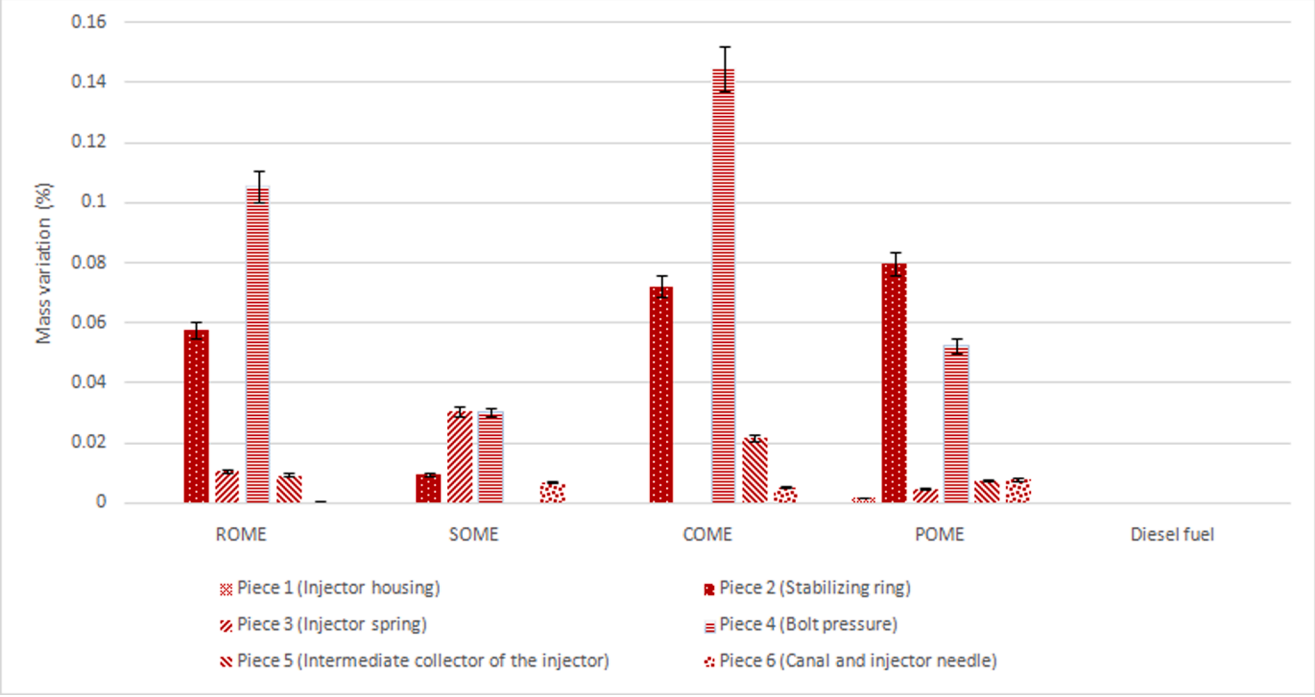

Fig. 2. Mass variation of pieces no. 1 to 6 (injector housing, stabilizing ring, injector spring, pressure bolt, injector intermediate collector and canal and injector needle, respectively). ROME: rapeseed oil methyl ester; SOME: soybean oil methyl ester; COME: coconut oil methyl ester; POME: palm oil methyl ester.

Table 5
Statistical analysis of mass variation.

			Piece no. 1	Piece no. 2	Piece no. 3	Piece no. 4	Piece no. 5	Piece no. 6
ROME [1]	Before immersion test	Standard deviation	0.00002	0.00002	0.00003	0.0007	0.00003	0.0000346
	After immersion test	Standard deviation	0.00002	0.00005	0.00003	0.00002	0.00004	0.00001
SOME [2]	Before Immersion test	Standard deviation	0.00002	0.00001	0.00004	0.00001	0.000052	0.00002
	After immersion test	Standard deviation	0.0000265	0.00001	0.00004	0.00001	0.00003	0.0000361
COME [3]	Before immersion test	Standard deviation	0.00003	0.00002	0.00001	0.0000173	0.00001	0.00002
	After immersion test	Standard deviation	0.00002	0.00001	0.00001	0.00002	0.00006	0.00001
POME [4]	Before immersion test	Standard deviation	0.00001	0.00001		0.00001	0.00003	0.00002
	After immersion test	Standard deviation	0.00007	0.0002	0.00001		0.00001	0.00001
Diesel fuel	Before immersion test	Standard deviation	0.00014	0.00021	0.00005	0.00013	0.00014	0.00000
	After immersion test	Standard deviation	0.00001	0.00002		0.00002		

[1] ROME: rapeseed oil methyl ester.
[2] SOME: soybean oil methyl ester.
[3] COME: coconut oil methyl ester.
[4] POME: palm oil methyl ester. Pieces no. 1 to 6: injector housing, stabilizing ring, injector spring, pressure bolt, injector intermediate collector and canal and injector needle, respectively.

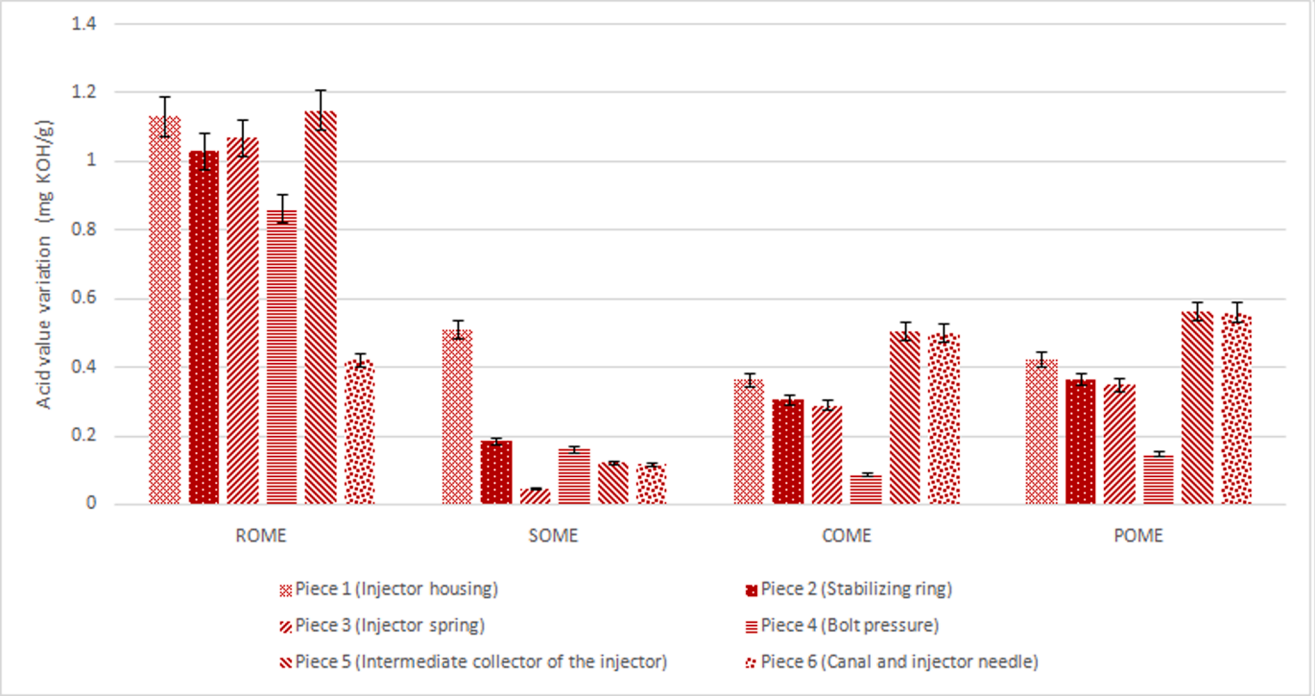

Fig. 3. Biodiesel acid value variation of pieces no. 1 to 6: injector housing, stabilizing ring, injector spring, pressure bolt, injector intermediate collector and canal and injector needle, respectively. ROME: rapeseed oil methyl ester; SOME: soybean oil methyl ester; COME: coconut oil methyl ester; POME: palm oil methyl ester.

used as oxide remover, inhibits granular growth and improves resistance to high temperature. Piece no. 5 included P, S, Cr and Mn. The presence of P improves machinability. Finally, piece no. 6 presented Si, Cr and Mn.

3.3. Injector piece mass variation

Once tests were finished, results shown that each injector piece immersed in biodiesel reduced its mass differently, depending on biodiesel type. Results concerning mass variation of each injector piece after tests is shown in Fig. 2. As may be seen, piece no. 1 was only affected by POME presence, while pieces no. 3 and 5 were not affected by COME and SOME, respectively. However, mass did not show any variation when those pieces were immersed in diesel fuel.

Pieces no. 2 and 4 are the ones that exhibited the highest loss of mass, highlighting those that have been immersed in COME (biodiesel with the lowest unsaturation degree and chain length) and ROME (among those biodiesel types with the highest unsaturation degree and length of chain). These pieces are the only ones that have Al as alloy. The least affected pieces were pieces no. 1, 3, 5 and 6, which do not contain Al. As previously mentioned, alloys act as catalysts to decompose biodiesel. Moreover, metals like Al, behave as catalysts for biodiesel oxidation. A summary of the statistics of the tests of mass variation, before and after immersion tests, is shown in Table 5. As may be seen, the low standard deviation values mean that most sample data are grouped close to its mean, which indicates very low dispersion.

3.4. Biodiesel acid value variation

Variation of biodiesel acid value after immersion tests is shown in Fig. 3. As can be seen, ROME showed a remarkable acid value increase for most pieces. On the contrary, SOME exhibited the lowest acid value variation for most pieces (excepting piece no. 1). ROME acid value did not meet European biodiesel standard EN 14214 threshold, excepting for piece no. 6. However, SOME and COME acid values remained below standard limit in all samples. POME only met standard considering

Table 6
Statistical analysis of acid value variation

	COME [1]		POME [2]		ROME [3]		SOME [4]	
	Standard deviation	Variance	Standard deviation	Variance	Standard deviation	Variance	Standard deviation	Variance
Blank	0.0957551	0.009169	0.0022968	0.0000052	0.1992309	0.0396929	0.0442282	0.0019561
Piece no. 1	0.0352132	0.0012399	0.0026533	0.0000070	0.0138249	0.0001911	0.0612125	0.0037469
Piece no. 2	0.0810578	0.0065703	0.0549486	0.0030193	0.1106481	0.012243	0.0621923	0.0038678
Piece no. 3	0.0131989	0.0001742	0.0069616	0.0000484	0.0176483	0.0003114	0.0584681	0.0034185
Piece no. 4	0.1944771	0.0378213	0.0130865	0.0001712	0.1098861	0.0120749	0.015726	0.0002473
Piece no. 5	0.0047772	0.0000228	0.0086035	0.0000745	0.0033365	0.0000111	0.0186323	0.0003471
Piece no. 6	0.0065064	0.0000423	0.0192456	0.0003703	0.0061598	0.0000379	0.0156054	0.0002435

[1] COME: coconut oil methyl ester.
[2] POME: palm oil methyl ester.
[3] ROME: rapeseed oil methyl ester.
[4] SOME: soybean oil methyl ester. Pieces no. 1 to 6: injector housing, stabilizing ring, injector spring, pressure bolt, injector intermediate collector and canal and injector needle, respectively.

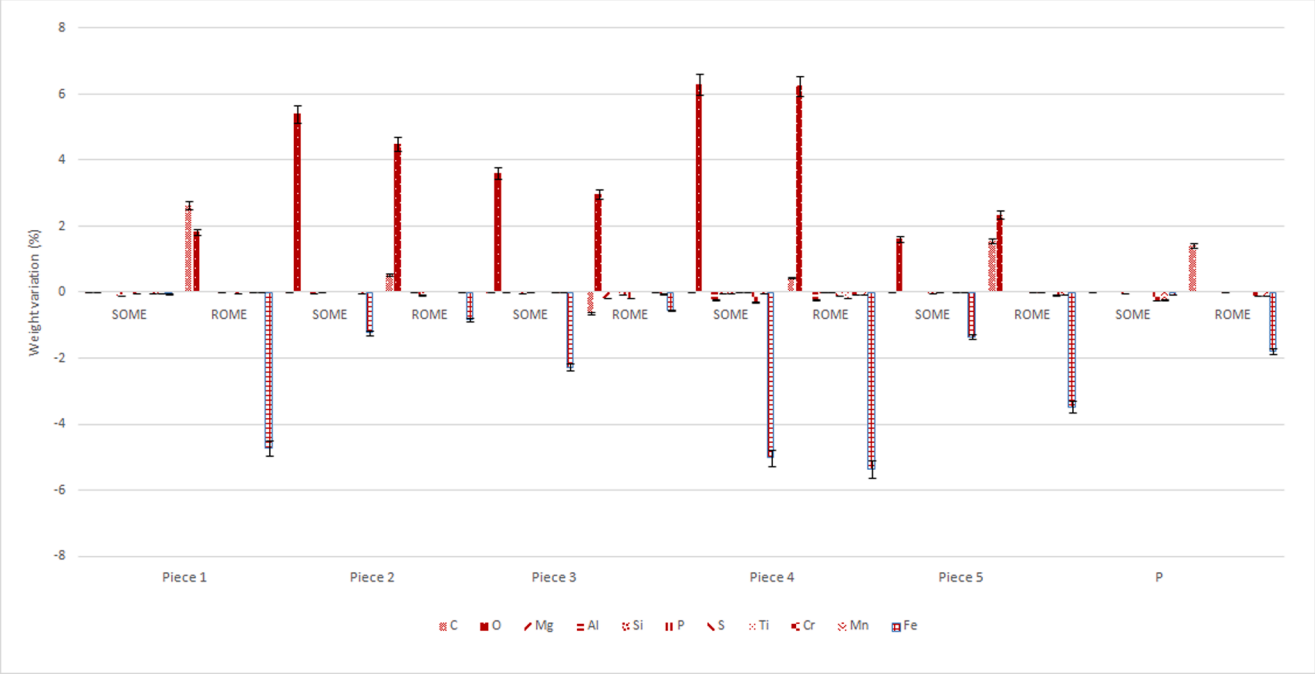

Fig. 4. Mass variation of elemental composition of pieces no. 1 to 6 (injector housing, stabilizing ring, injector spring, pressure bolt, injector intermediate collector and canal and injector needle, respectively) immersed in ROME (rapeseed oil methyl ester) and SOME(soybean oil methyl ester).

pieces no. 1, 2 and 3. COME and POME, produced from the most unsaturated oils, exhibited a similar behavior.

As may be seen, tests carried out with piece no. 4 provided the lowest increase in biodiesel acid value. It seems that Ti is less reactive with biodiesel compared to other metals. This piece is the only one that has Ti as alloying element, although it is also the one that includes the highest number of alloying elements in its internal structure (Table 4). A summary of the statistics considering acid value variation is shown in Table 6, also, showing very low data dispersion.

3.5. Weight variation for pieces immersed in ROME and SOME

As mentioned in the methodology section, for being the most and less outstanding in terms of acid value increase, respectively, pieces immersed in ROME and SOME were analyzed after immersion tests, by EDS. Mass variation after tests is shown in Fig. 4, where negative values indicate material loss. As may be seen, the presence of oxygen stood out, possibly due to the formation of metal oxides. Also, an increase in carbon was found. This is possibly due to environmental contamination and potential biodiesel residues in metal pieces, despite the washing step. However, other elements expected to be in suspension decreased, mainly Fe (showing the most significant losses), as they settled down at the bottom of biodiesel sample jars.

3.6. Metal surface analysis by XPS

As it was the most outstanding case of study result, after completion of immersion test, corrosion of piece no. 2 immersed in SOME was further analyzed by XPS (Al-X-ray 1486.6 eV). Surface corrosion was generally visible as brown spots, a state associated with a rough surface finish. Since the beginning of the analysis, the presence of Fe, Mn, O and C stood out as shown in Fig. 5. These detected elements were in either solid state, dissolved or forming compounds, since the equipment works under high vacuum. At each sweep stage, compounds were detected by their binding energy (Figs. 5 and 6).

Mn, usually present in all steels, is used to neutralize the pernicious influence of sulfur and oxygen, that liquid steels normally contain. To delve into the layers of atom closest to the surface, an Ar sweep was performed for 10 min and data were collected. Then, another 20 min sweep was performed. The binding energy showed the existence of

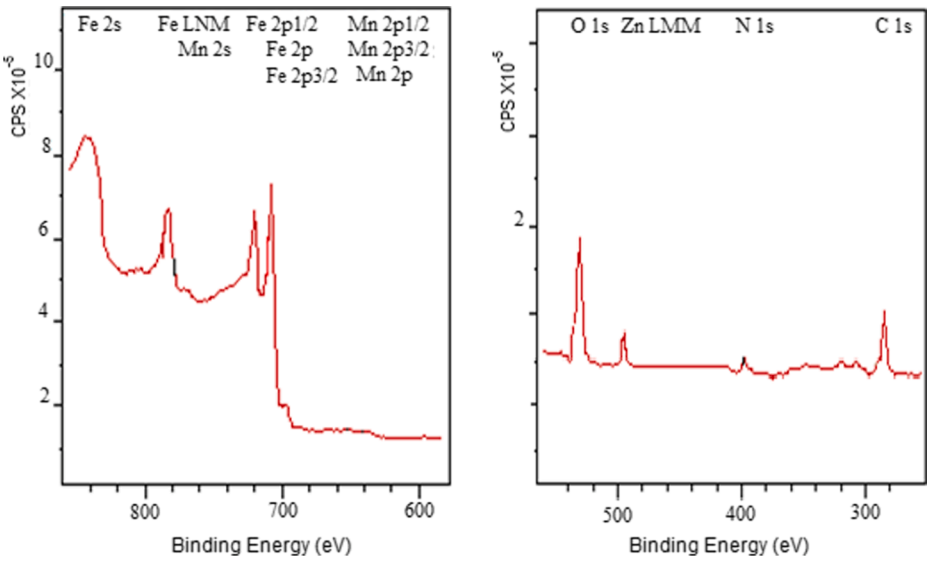

Fig. 5. Presence of Fe, Mn, O and C in piece no. 2, immersed in soybean oil methyl ester for 1100 h, at room temperature.

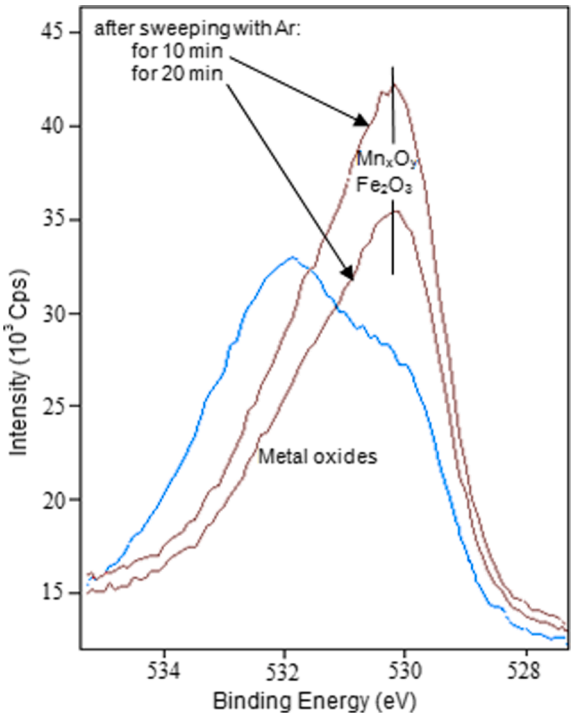

Fig. 6. Presence of Mn_2O_3 (529.6 eV), MnO (529.7 eV), MnO_2 (530 eV), Fe_2O_3(530 eV) and other metal oxides (528–532 eV) in piece no. 2, immersed in soybean oil methyl ester for 1100 h, at room temperature.

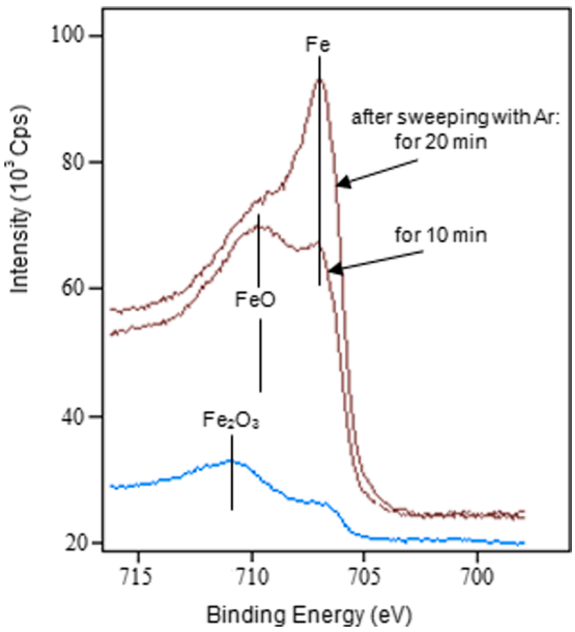

Fig. 7. Presence of Fe (707 eV), FeO (709 eV) and Fe_2O_3 (711 eV) in piece no. 2, immersed in soybean oil methyl ester for 1100 h, at room temperature.

Mn_2O_3 (529.6 eV), MnO (529.7 eV), MnO_2 (530 eV), Fe_2O_3 (530 eV) and other metal oxides (528–532 eV), as can be seen in Fig. 6. Fe (707 eV), FeO (709 eV) and Fe_2O_3 (711 eV) were also detected as shown in Fig. 7. As it deepened, Fe oxides (Fe_xO_y) gave place to Fe.

4. Conclusions

Results from visual inspection show different corrosion depending on both, fuel type and piece composition. In general terms, either the lower the chain length or the lower the unsaturation degree, the lower the color tone change. However, not a clear trend of biodiesel fatty acid composition influence over material corrosion was found. In fact, rapeseed and soybean oil methyl esters (highest unsaturation degree and chain length) provided the highest and lowest acidity increase, respectively. After immersion tests, mainly oxides of Mn and Fe were found in metallic pieces, indicating corrosion issues. Considering mass changes, presence of aluminum provided the worst results. In conclusion, biodiesel degradation and material corrosion were beyond European biodiesel standard EN 14214 parameters, that only include copper band corrosion. Alloys require a corrosion study in depth. To promote changes in biodiesel standard, further research on actual engine parts, including both static and dynamic tests, is recommended.

CRediT authorship contribution statement

A. Alcántara-Carmona: Investigation, Methodology, Writing - original draft. **F.J. López-Giménez:** Methodology, Supervision. **M.P. Dorado:** Conceptualization, Visualization, Methodology, Writing -

review & editing.

Declaration of Competing Interest

The authors declare that they have no known competing financial interests or personal relationships that could have appeared to influence the work reported in this paper.

Acknowledgement

This research was developed thanks to the support of the Spanish Ministries of Economy and Competitiveness (ENE2013-47769-R) and Science and Research (PID2019-105936RB-C21), respectively. Funding for open access charge: Universidad de Córdoba / CBUA.

Appendix A. Supplementary data

Supplementary data to this article can be found online at https://doi.org/10.1016/j.fuel.2021.121788.

References

[1] Ideris F, Shamsuddin AH, Nomanbhay S, Kusumo F, Silitonga AS, Ong MY, et al. Optimization of ultrasound-assisted oil extraction from *Canarium odontophyllum* kernel as a novel biodiesel feedstock. J Clean Prod 2021;288:125563. https://doi.org/10.1016/j.jclepro.2020.125563.
[2] Silitonga AS, Shamsuddin AH, Mahlia TMI, Milano J, Kusumo F, Siswantoro J, et al. Biodiesel synthesis from *Ceiba pentandra* oil by microwave irradiation-assisted transesterification: ELM modeling and optimization. Renew Energy 2020;146:1278–91.
[3] Ong HC, Milano J, Silitonga AS, Hassan MH, Shamsuddin AH, Wang C-T, et al. Biodiesel production from *Calophyllum inophyllum-Ceiba pentandra* oil mixture: Optimization and characterization. J Clean Prod 2019;219:183–98.
[4] Pinzi S, Garcia IL, Lopez-Gimenez FJ, Luque de Castro MD, Dorado G, Dorado MP. The ideal vegetable oil-based biodiesel composition: A review of social, economical and technical implications. Energ Fuels 2009;23(5):2325–41.
[5] Jain S, Sharma MP. Stability of biodiesel and its blends: A review. Renew Sustain Energy Rev 2010;14(2):667–78.
[6] Knothe G, Dunn RO. Dependence of oil stability index of fatty compounds on their structure and concentration and presence of metals. J Am Oil Chem Soc 2003;80(10):1021–6.
[7] Sarin A, Arora R, Singh NP, Sharma M, Malhotra RK. Influence of metal contaminants on oxidation stability of Jatropha biodiesel. Energy 2009;34(9):1271–5.
[8] Sarin A, Arora R, Singh NP, Sarin R, Malhotra RK. Oxidation stability of palm methyl ester: Effect of metal contaminants and antioxidants. Energ Fuels 2010;24(4):2652–6.
[9] Linhares FN, Senra Gabriel CF, Furtado de Sousa AM, Amorim Moreira Leite MC, Guimaraes Furtado CR. Nitrile rubber and carboxylated nitrile rubber resistance to soybean biodiesel. Polimeros-Ciencia E Tecnologia 2018;28(1):23–9.
[10] Komariah LN, Arita S, Aprianjaya F, Novaldi MG, Fathullah MF, Polytechn Sriwijaya PSSI. O-Rings material deterioration due to contact with biodiesel blends in a dynamic fuel flow. 2nd Forum in Research, Science, and Technology. 2019.
[11] Komariah LN, Hadiah F, Aprianjaya F, Nevriadi F. Biodiesel effects on fuel filter; assessment of clogging characteristics. In: 6th International Conference of the Indonesian Chemical Society; 2018. p. 012017. https://doi.org/10.1088/1742-6596/1095/1/012017.
[12] Gulzar M, Masjuki HH, Varman M, Kalam MA, Zulkifli NWM, Mufti RA, et al. Effects of biodiesel blends on lubricating oil degradation and piston assembly energy losses. Energy 2016;111:713–21.
[13] Chen B, Wang J, He T, Jie F, Chen B. Impact of biodiesel on engine oil quality: Role of methyl oleate and performance of sulfonate detergent additive. Fuel 2019;244:454–60.
[14] Almeida ES, Portela FM, Sousa RMF, Daniel D, Terrones MGH, Richter EM, et al. Behaviour of the antioxidant tert-butylhydroquinone on the storage stability and corrosive character of biodiesel. Fuel 2011;90(11):3480–4.
[15] Jakeria MR, Fazal MA, Haseeb ASMA. Effect of corrosion inhibitors on corrosiveness of palm biodiesel. Corros Eng Sci Technol 2015;50(1):56–62.
[16] Fazal MA, Sazzad BS, Haseeb ASMA, Masjuki HH. Inhibition study of additives towards the corrosion of ferrous metal in palm biodiesel. Energ Convers Manage 2016;122:290–7.
[17] Haseeb ASMA, Masjuki HH, Ann LJ, Fazal MA. Corrosion characteristics of copper and leaded bronze in palm biodiesel. Fuel Process Technol 2010;91(3):329–34.
[18] Fazal MA, Haseeb ASMA, Masjuki HH. Comparative corrosive characteristics of petroleum diesel and palm biodiesel for automotive materials. Fuel Proces Technol 2010;91(10):1308–15.
[19] Hu E, Xu Y, Hu X, Pan L, Jiang S. Corrosion behaviors of metals in biodiesel from rapeseed oil and methanol. Renew Energy 2012;37(1):371–8.
[20] Norouzi S, Eslami F, Wyszynski ML, Tsolakis A. Corrosion effects of RME in blends with ULSD on aluminium and copper. Fuel Process Technol 2012;104:204–10.
[21] McCormick RL, Ratcliff M, Moens L, Lawrence R. Several factors affecting the stability of biodiesel in standard accelerated tests. Fuel Process Technol 2007;88(7):651–7.
[22] Fazal MA, Haseeb ASMA, Masjuki HH. Effect of temperature on the corrosion behavior of mild steel upon exposure to palm biodiesel. Energy 2011;36(5):3328–34.
[23] Chandran D. Compatibility of diesel engine materials with biodiesel fuel. Renew Energy 2020;147:89–99.
[24] Sorate KA, Bhale PV. Corrosion behavior of automotive materials with biodiesel: A different approach. SAE Int J Fuels Lubr 2018;11(2):147–62.
[25] Chandran D, Ng HK, Lau HLN, Gan S, Choo YM. Deterioration of palm biodiesel fuel under common rail diesel engine operation. Energy 2017;120:854–63.
[26] Pinzi S, Mata-Granados JM, Lopez-Gimenez FJ, Luque de Castro MD, Dorado MP. Influence of vegetable oils fatty-acid composition on biodiesel optimization. Bioresour Technol 2011;102(2):1059–65.
[27] Sáez-Bastante J, Pinzi S, Arzamendi G, Luque de Castro MD, Priego-Capote F, Dorado MP. Influence of vegetable oil fatty acid composition on ultrasound-assisted synthesis of biodiesel. Fuel 2014;125:183–91.